Analysis of Ocean Heat Content Change in ENACT and Study into the effect of data Sampling Resolution on an Eddy-permitting Ocean Model (HadCEM)

Hadley Centre technical note 58

Lesley Allison

15 November 2004

Analysis of Ocean Heat Content Change in ENACT, and Study into the Effect of Data Sampling Resolution on an Eddy-permitting Ocean Model (HadCEM)

Lesley Allison
Department of Meteorology, University of Reading, UK
E-mail: swu02lca@reading.ac.uk

1. Introduction

This report is the result of a 6 week Industrial Scholarship placement (12th July – 20th August 2004) at the Met Office. The work was supervised by Michael Vellinga and Helene Banks in the department of Ocean Applications.

The change in ocean heat content over the past 44 years is studied using an objective analysis of ocean temperature observations. It was produced in the Met Office under the ENACT (ENhanced ocean data Assimilation and Climate predicTion) project. The ENACT program was conducted by a number of organisations from several European countries. One aim of ENACT was to quality control historical ocean observations from a range of sources including the World Ocean Database 2001 (WOD01) and improve the observation processing system. The ENACT analyses used are produced without a forecast model, using damped persistence of the monthly analysis anomalies and relaxing towards Levitus climatology (the average for each month) in the absence of any observations. The ENACT objective analysis is described in detail by Ingleby and Huddleston (2004). The objective analysis is the source of data for the first part of this report, and will be further referred to as 'ENACT'.

The trend in ocean heat content and associated temporal variability over the world ocean in ENACT are compared to analyses by Levitus et al. (2000), and results from the HadCM3 coupled atmosphere-ocean general circulation model (AOGCM), as presented by Gregory et al. (2004). The climate model HadCM3 is described in detail by Gordon et al. (2000) The results from Levitus et al. (2000) will hereafter be referred to as the "Levitus" results. It is found that the trend in heat content from the ENACT reanalysis is comparable with Levitus and HadCM3, and that the temporal variability is similar to that seen in the Levitus time-series.

The heat content trend and variability are studied for separate regions of the world ocean, and at various depths.

In section 3 the effect of sub-sampling on an eddy-permitting ocean model (HadCEM) is investigated. HadCEM (Hadley Centre Coupled Eddy-permitting Model) has a horizontal resolution of 1/3˚, and 40 vertical levels. It is found that spatial sub-sampling introduces spurious variability to the ocean temperature time-series and between multiple realisations.

Finally, improvements and possibilities for further work are suggested.

2. Analysis of Ocean Heat Content Change in ENACT objective analysis

2.1 Global Trend in Ocean Heat Content

Analysis of ocean heat content time-series of ENACT has shown an overall increase since 1958. Figure 1 shows the time-series of ocean heat content anomaly over the global domain. The annual mean trend is $0.41 \pm 0.06 \times 10^{22}$ Jyr^{-1}, where the error residual is given by one standard error of the trend. A comparison between this result,

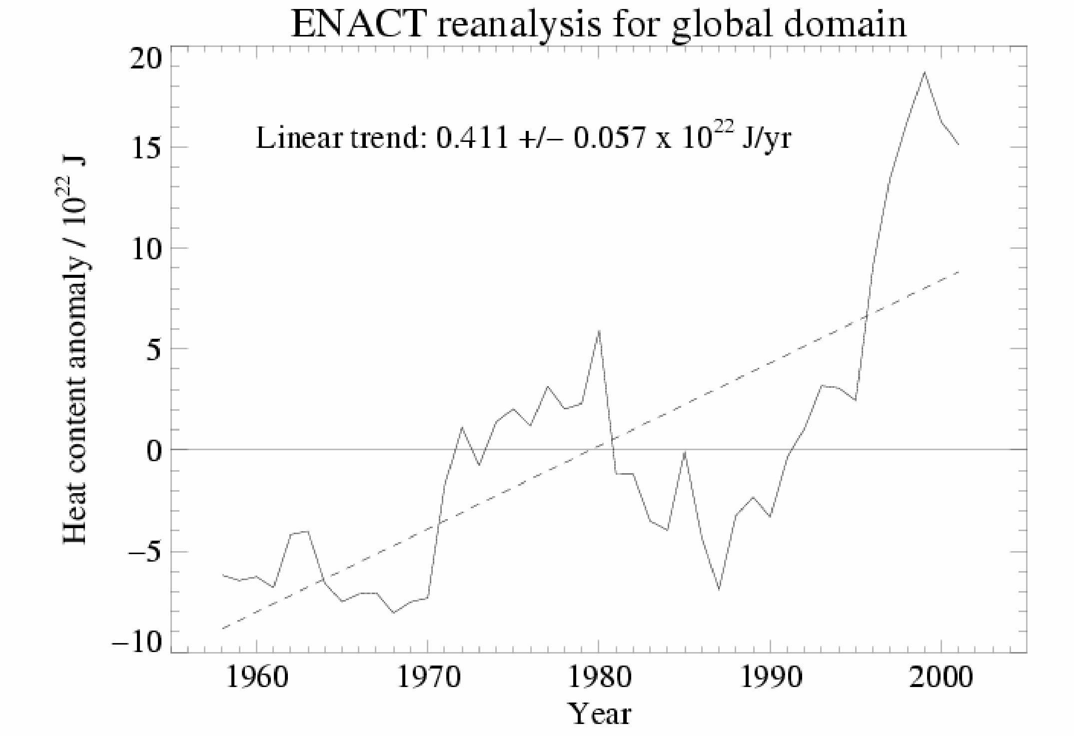

the values obtained by Levitus and various forced experiments with the HadCM3 AOGCM is given in Table 1.

Table 1. Comparisons of ocean heat content trend (Jyr^{-1}) between ENACT, HadCM3 and the Levitus time-series. Values taken from Gregory et al., 2004

	Heat content trend (Jyr^{-1})
ENACT	$0.41 \pm 0.06 \times 10^{22}$
Levitus	$0.32 \pm 0.04 \times 10^{22}$
HadCM3 (Greenhouse gases only)	0.62×10^{22}
HadCM3 (Natural, i.e. solar + volcanic)	-0.07×10^{22}
HadCM3 (Anthropogenic aerosols + greenhouse gases)	0.23×10^{22}
HadCM3 (All forcings)	0.16×10^{22}

Fig. 1. Time-series of heat content anomaly (10

The trend exhibited by ENACT is greater than all but one of the other trends. The only value that is larger than that from ENACT is from the greenhouse gases ensemble-member of HadCM3. The trend value in ENACT is influenced by a sharp increase in heat content after 1995. This period is not included in the Levitus time-series (which runs from 1955 to 1995), and hence the increase does not contribute to the Levitus trend. This may start to explain why the trend in ENACT is lower than in Levitus. Despite this, when the error residuals are taken into account, the trends from ENACT and Levitus are comparable.

2.2 Decadal Variability

Gregory et al. (2004) looked in detail into decadal variability superimposed on the upward trend in the Levitus time-series, and found that HadCM3 did not reproduce this variability. Figure 2 shows the comparison between these two results and the ENACT time-series.

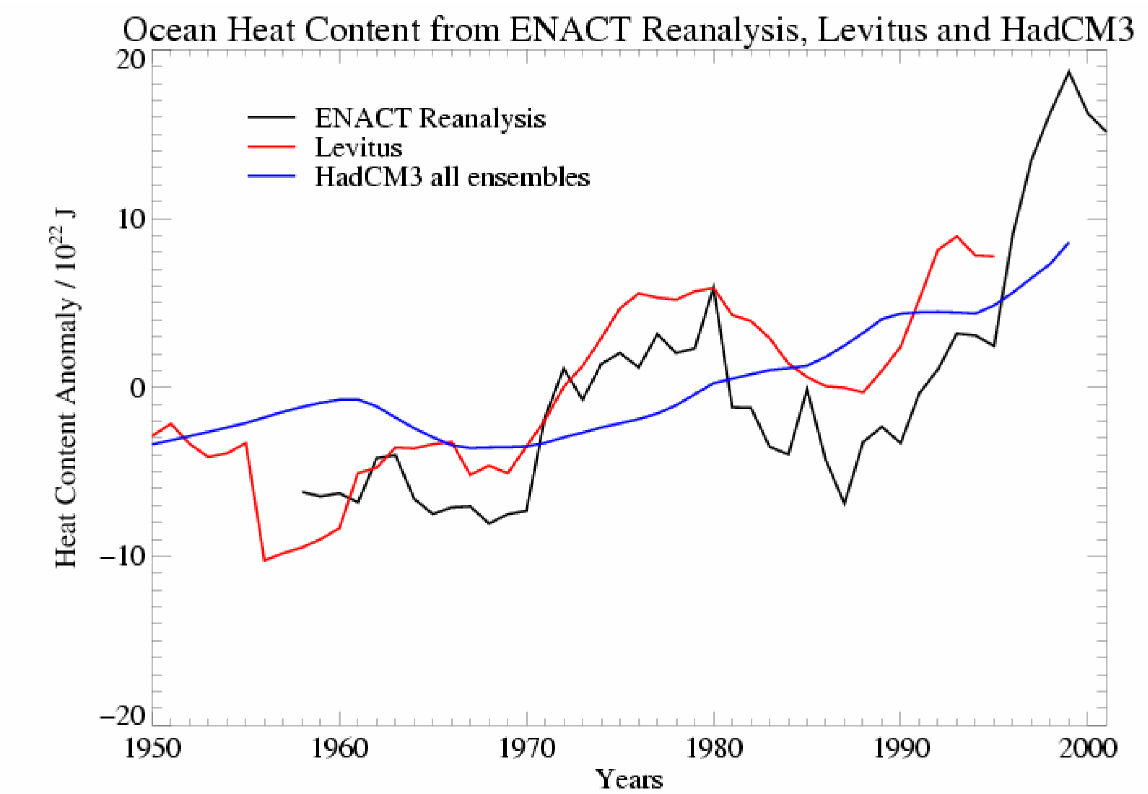

Fig. 2. Comparison between ocean heat content time-series from ENACT, Levitus and HadCM3 (all forcings ensemble). Adapted from Gregory et al., 2004, their Figure 1.

The ENACT reanalysis exhibits decadal variability comparable with the Levitus results. The warming and cooling phases coincide. The systematic offset between ENACT and Levitus is probably due to the sharp increase in heat content observed in ENACT at the end of the time-series. As the plot shows heat content anomalies rather than absolute values, this large value at the end causes the rest of the time-series to be lower. After 1960, the value of the ENACT time-series is lower than the Levitus time-series at almost every point. As pointed out by Gregory et al. (2004), the trend in heat content anomaly in HadCM3 is similar to the other time-series, but the decadal variability is not reproduced in the model.

2.3 Temperature Change in Sub-Regions of the Ocean

From the value of heat content, the mean temperature trend for the global ocean was found to be $1.33 \pm 0.18 \times 10^{-3}$ Kyr^{-1}. The world ocean was divided into separate ocean basins, latitudinal strips (60˚ wide) and vertical layers. The temperature changes were calculated for each region. The ocean basin which exhibits the largest trend is the Atlantic, with a value of $2.22 \pm 0.26 \times 10^{-3}$ Kyr^{-1}. The Indian Ocean yields a similar value of $1.96 \pm 0.24 \times 10^{-3}$ Kyr^{-1}. The largest trend in the latitudinal strips is found in the tropics (30˚N to 30˚S), where the value is $1.58 \pm 0.18 \times 10^{-3}$ Kyr^{-1}. The uppermost of the vertical layers (top 100m) exhibits the largest trend of $6.30 \pm 0.80 \times 10^{-3}$ Jyr^{-1}.

The change in temperature trend with depth is given in Figure 3. The error bars indicate one standard error. The observed temperature trend is greater towards the ocean surface, and decays monotonically with depth. This may be due to greater mixing in the surface layers, caused by wind stress and weaker density gradients. The warmed surface water may only be transported a small depth by mixing, leading to the observed decay in temperature change with depth.

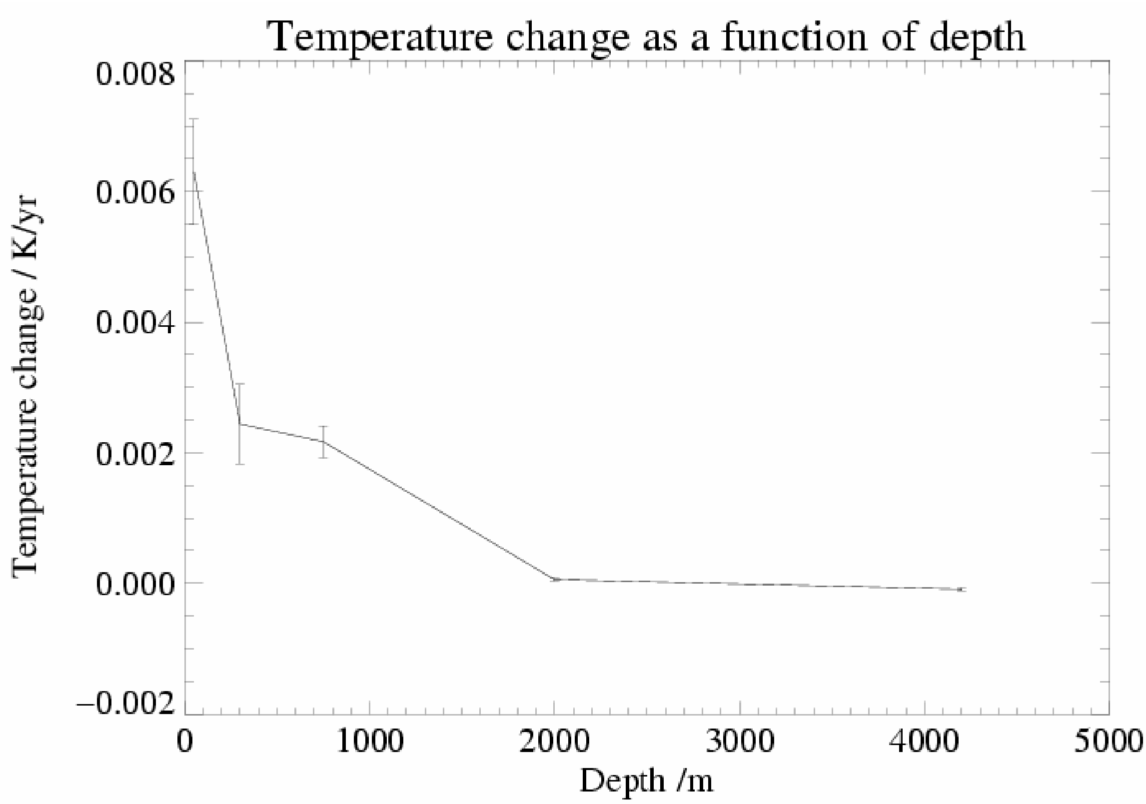

Fig. 3. Temperature change as a function of depth (ENACT, 1958-2001). The error bars represent one standard error. The water column was split into 5 levels of varying thickness, and the temperature trend was calculated for each level.

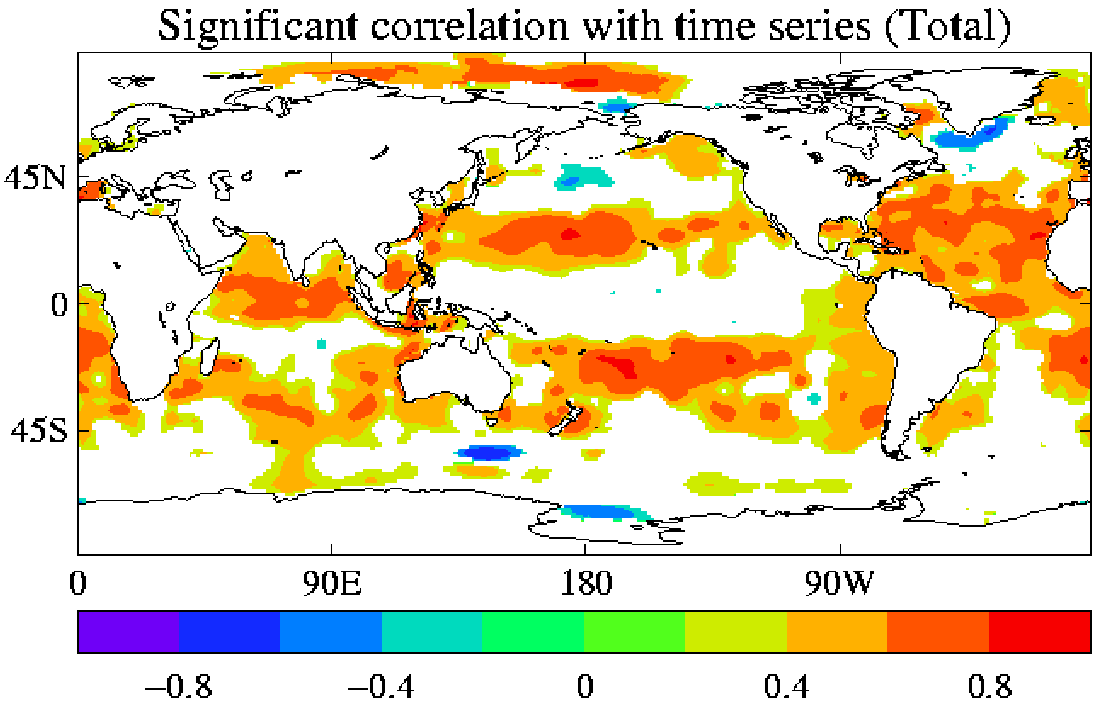

Fig. 4. Regions with significant correlation with global time-series (ENACT, 1958-2001)

To determine which regions of the world ocean contributed most to the observed trend, a plot was constructed to show areas of significant correlation with the global time-series (Fig.4). Areas of positive correlation can be found in the Subtropical Atlantic and Pacific, Indian Ocean and Arctic Ocean. Small regions of negative correlation are located south of Greenland, in the North Pacific and in the Ross Sea. In the North Atlantic and Pacific, parts of the Tropics and in the Southern Ocean there is no correlation. It is interesting to note that although the North Atlantic is an area with a relatively high sampling density, it shows little or no correlation with the global time-series. This suggests that a physical reason, rather than the effect of sub-sampling (see section 1.5), may be causing the low correlation. An example of a physical cause of the lack of correlation in the North Atlantic is a change in the thermohaline circulation. The lack of correlation in the tropical Pacific may be the result of ENSO. The changes in sea surface temperature in this region associated with ENSO may have obscured the warming trend seen in the majority of the world ocean.

2.4 Temperature Variability with Depth

Figure 5 shows the profile of temperature variability with depth. Following Gregory et al. 2004, the data was detrended to remove the warming signal, and smoothed using five-year running means. In the analysis of this figure, it will be compared to the variability in the Levitus results as a function of depth (Gregory et al., 2004, their Figure 4). The ENACT variability decreases with depth, with a maximum around 50-60m as observed in the Levitus results. There is rather more noise in the variability trend in the ENACT data in comparison to the Levitus data. An obvious feature of the Levitus variability is a strong maximum at a depth of 500m. This is not evident in

ENACT. In ENACT the variability remains high, down to a depth of 400m, after which it decreases sharply. There is a small peak at 800-900m. The peak at 500m observed in the Levitus results is most evident in the Tropics (30˚N to 30˚S). The variability in ENACT was studied for the tropical sub-region (Fig.5 right-hand panel), but this feature was still not observed.

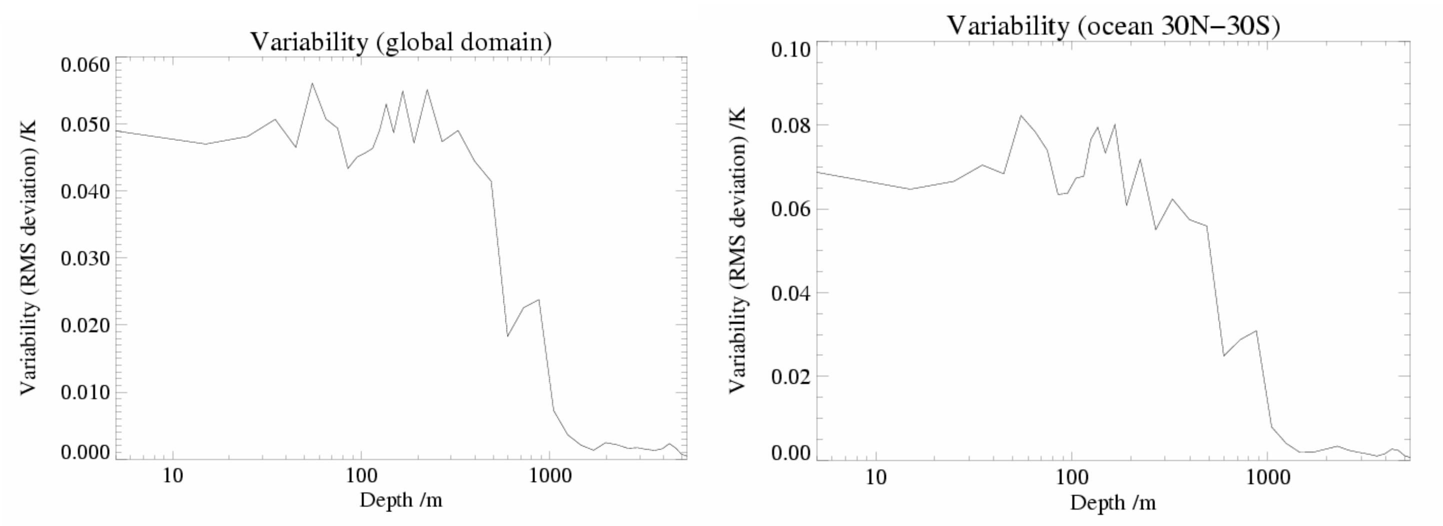

Fig. 5. Temperature variability as a function of depth for the global domain and the Tropics (30˚N to 30˚S). The variability is given by the RMS deviation from the mean. The data has been detrended and smoothed using five-year running means.

2.5 The Effect of Data Sampling

An important factor to consider with any observational dataset is the sampling density. In the interior of the ocean, spatial and temporal data coverage is rather sparse. This introduces uncertainty in the results, the extent of which is not clear. In the ENACT dataset the sampling density is greatest in the northern hemisphere upper ocean, and is mostly restricted to shipping lanes. It is greater in recent years and decreases with depth. Figure 6 is taken from a presentation by Bruce Ingleby and shows the number of ENACT observations with time and depth.

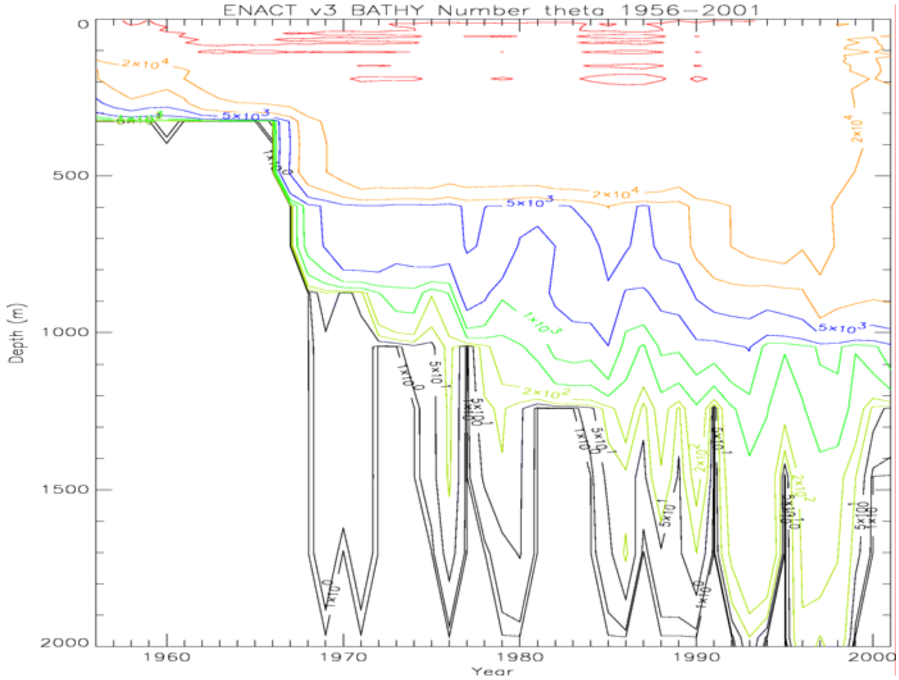

Fig. 6. Incidence of ENACT observations taken by mechanical and expendable bathythermographs against time and depth. These form the bulk, but not all, of the available observations (Ingleby and Huddleston, ENACT, 2004)

Interpolation methods are used to fill gaps in the data. In the ENACT dataset a finite radius of influence is assigned to each data point. The value of the parameter measured at that point (e.g. temperature) decays with distance from the point, as well as with time. This produces a smoothed anomaly field.

The result of this interpolation method is that areas with a low sampling density have fewer points to contribute to the large-scale heat content anomaly. This may cause these areas to have a lower value of heat content, and may explain the lack of correlation seen in the sparsely sampled Southern Ocean in Figure 4.

The next section of this report addresses the issue of spatial sampling density in a climate model with fine resolution in the ocean.

3. The Sensitivity of HadCEM to Data Sampling Resolution

3.1 The Motivation for a High Resolution Ocean Model

The resolution of climate models is restricted by the available computer resources, and it is recognised that atmospheric models with a resolution of around 300km are able to represent the basic circulation features (Roberts et al., 2003). However, ocean circulation features, such as baroclinic eddies, often exist on a much smaller scale and are not well represented in current climate models.

In the context of calculating the ocean heat content from observations taken at disrete points, eddy activity can be very important. High temperature gradients are associated with ocean eddies, which means that spurious temperature results can be obtained if the sampled point lies within an eddy. A higher resolution model can take eddy activity into account.

HadCEM (Hadley Centre Coupled Eddy-permitting Model) has an ocean resolution of 1/3˚, and can resolve small-scale oceanic flows. There are 40 vertical levels of varying thickness. The integration used in this study runs for 30 years with a 2% yr^{-1} increase in CO_2, starting at pre-industrial levels. The data we used are monthly-averaged values of ocean temperature.

3.2 Simulated Change in Ocean Heat Content in HadCEM

Figure 7 shows the global mean temperature anomaly for the upper 3000m from HadCEM. The CO_2 forcing has caused an exponential increase in global ocean temperature. The seasonal temperature cycle is clearly visible.

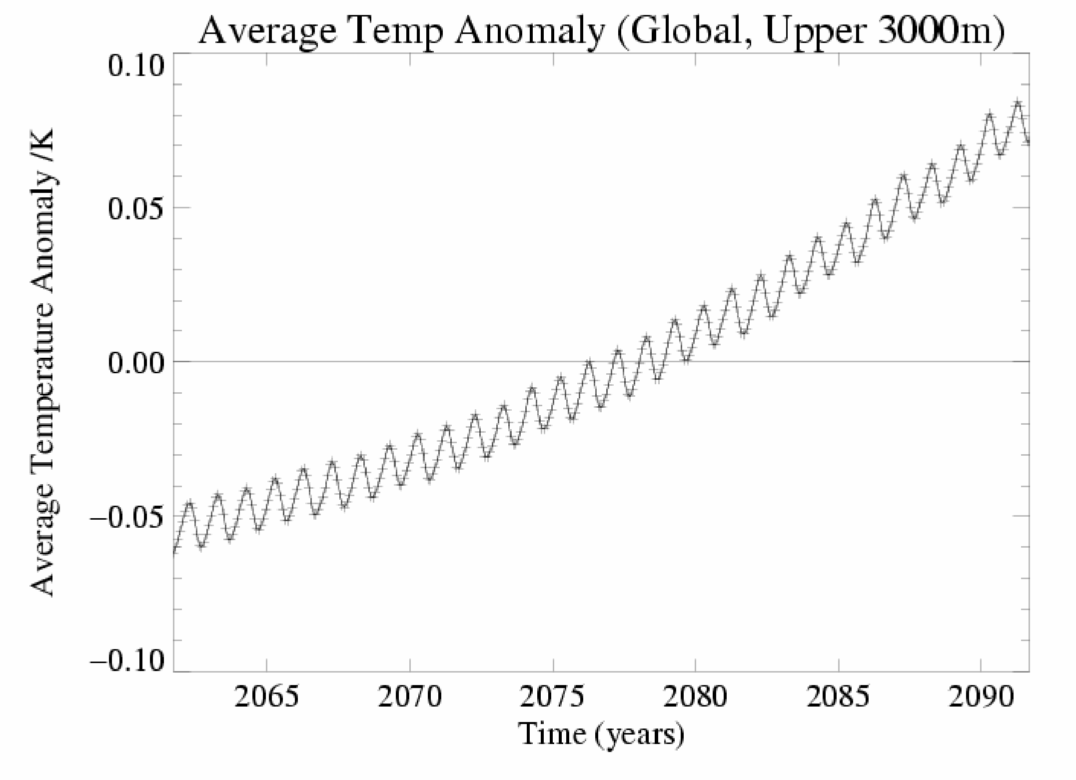

Fig. 7. Simulated global mean temperature anomaly for upper 3000m (HadCEM). The values on the time axis do not correspond to the years marked. The run starts nominally at 2061 with pre-industrial levels of CO_2 and extends for 30 years.

3.3 Explanation of Sub-sampling Method

The effect of sub-sampling was studied in HadCM3 by Palmer and Banks (2004). It was found that by sampling the ocean at coarser resolutions, variability in potential temperature is increased. The effect that sub-sampling has in the context of an eddy-permitting ocean model will now be investigated.

To simulate the effect of sampling at a coarser resolution, the data from the fine resolution HadCEM run was sub-sampled spatially at a range of resolutions. The original grid contains 1080 x 540 grid boxes (1/3˚ resolution). To obtain a sampling resolution of 1˚, the original grid was looped over in steps of 3 grid boxes. For 2˚ resolution, it was looped over in steps of 6, and so on. The data was sub-sampled at resolutions of 1˚, 2˚, 3˚, 4˚ and 5˚. This produced a fewer number of larger grid boxes.

The temperature value within each of these larger grid boxes was determined by randomly selecting one of the small grid boxes contained within it, and taking its value to be representative for the entire large grid box. The location of the representative small grid box was used at every depth level at that horizontal position. This gave the effect of dropping a device into the ocean at that location and measuring values of temperature at varying depths as the device descended, thereby making the sub-sampling technique as close to reality as possible.

This method was repeated to obtain 4 realisations, taking a different randomly selected small grid box each time. This had the effect of sampling the variability resulting from taking particular locations of the chosen small grid box.

Initial results indicated that some changes had to be made to the sub-sampling method. In the temperature time-series there was a systematic offset between some of the realisations. This may have been because the original method caused the volume of the ocean to be changed, depending on the position of the selected small grid box. Near the coast, in a large grid box containing several small grid boxes, some of these small boxes are sea points and some are land points. Originally, homogenising the large grid box by selecting one of the small boxes and making all the others equal to the value of the selected one could therefore change the type of some of the boxes. If a sea point was selected, the land points within the large grid box would become sea points, and hence the volume of the ocean in that grid box would increase. The modified method kept the sea and land points separate. One small grid box was selected from the sea points only, and its value was assumed for all the remaining sea points in the large grid box. The land points remained unchanged. This preserved the correct shape of the coastline, and hence helped to prevent changes to the ocean's volume.

An additional feature of the modified method was a depth check. Before a small grid box was accepted, its depth was checked to confirm that there would be a sufficient number of vertical readings. If the depth of the selected point exceeded 75% of the mean depths of small grid boxes within the large grid box, then it was accepted.

The modifications made to the sub-sampling method appeared to be successful. Before the modifications half of the realisations were offset from the mean, whereas afterwards none were offset.

3.4 The Effects of Sub-sampling at Coarser Resolutions

Figure 8 shows 4 realisations of global mean temperature anomaly from HadCEM, sub-sampled at a resolution of 5˚. While the trend and the absolute values of temperature are consistent for each resolution, the coarser resolution has introduced variability to each time-series that differs between the realisations.

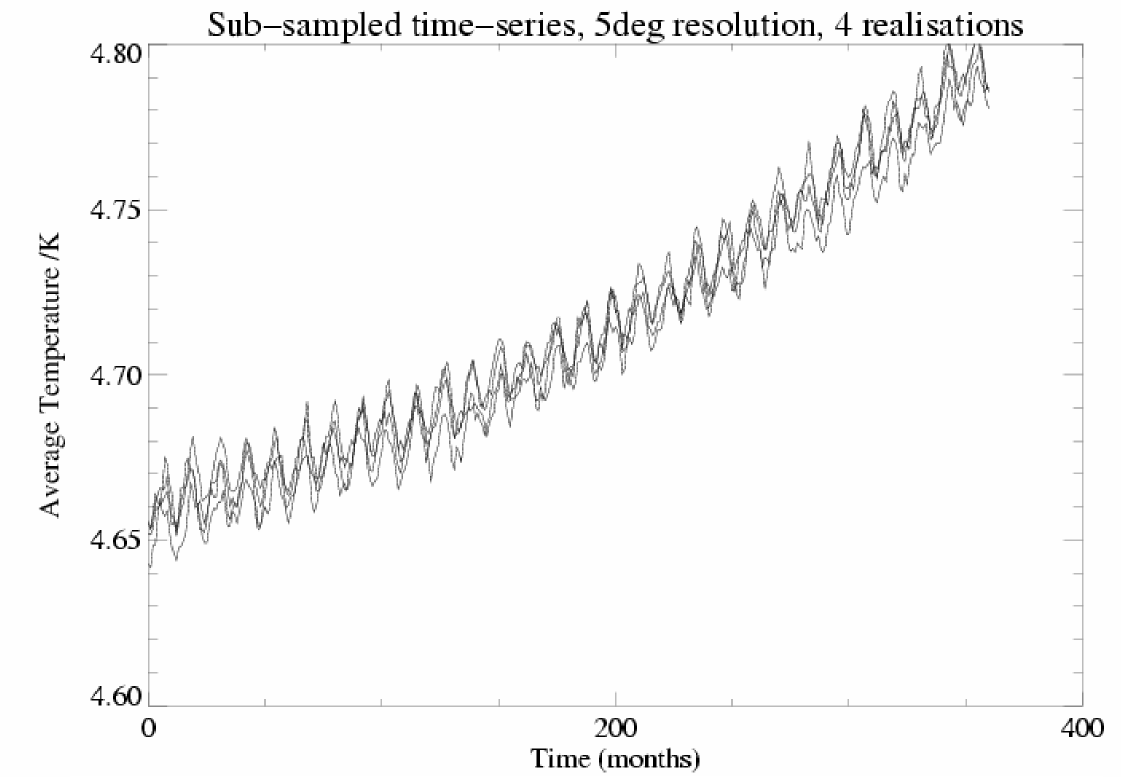

Fig. 8. Global mean temperature anomaly from HadCEM, sub-sampled at a resolution of 5˚ (4 realisations)

To quantitatively compare the temperature variability for different resolutions, the warming trend and the seasonal variability were removed. The mean of the four realisations was calculated, and this was detrended using a quadratic fit (as this was close to the exponential trend observed). Monthly climatology was calculated by taking the mean values for each month. The seasonal cycle was then removed by subtracting the monthly climatology from each month's value. Figure 9 shows the result of the detrending and smoothing for 5˚ resolution.

The RMS variability was calculated for each of the resolutions studied, and the results are shown in Figure 10. It is clear that increasing the spatial resolution of the model leads to an increase in the temperature variability. This is consistent with the findings of Palmer and Banks. The increase appears to be non-linear, so that at fine resolution a small increase in resolution leads to a relatively large increase in variability.

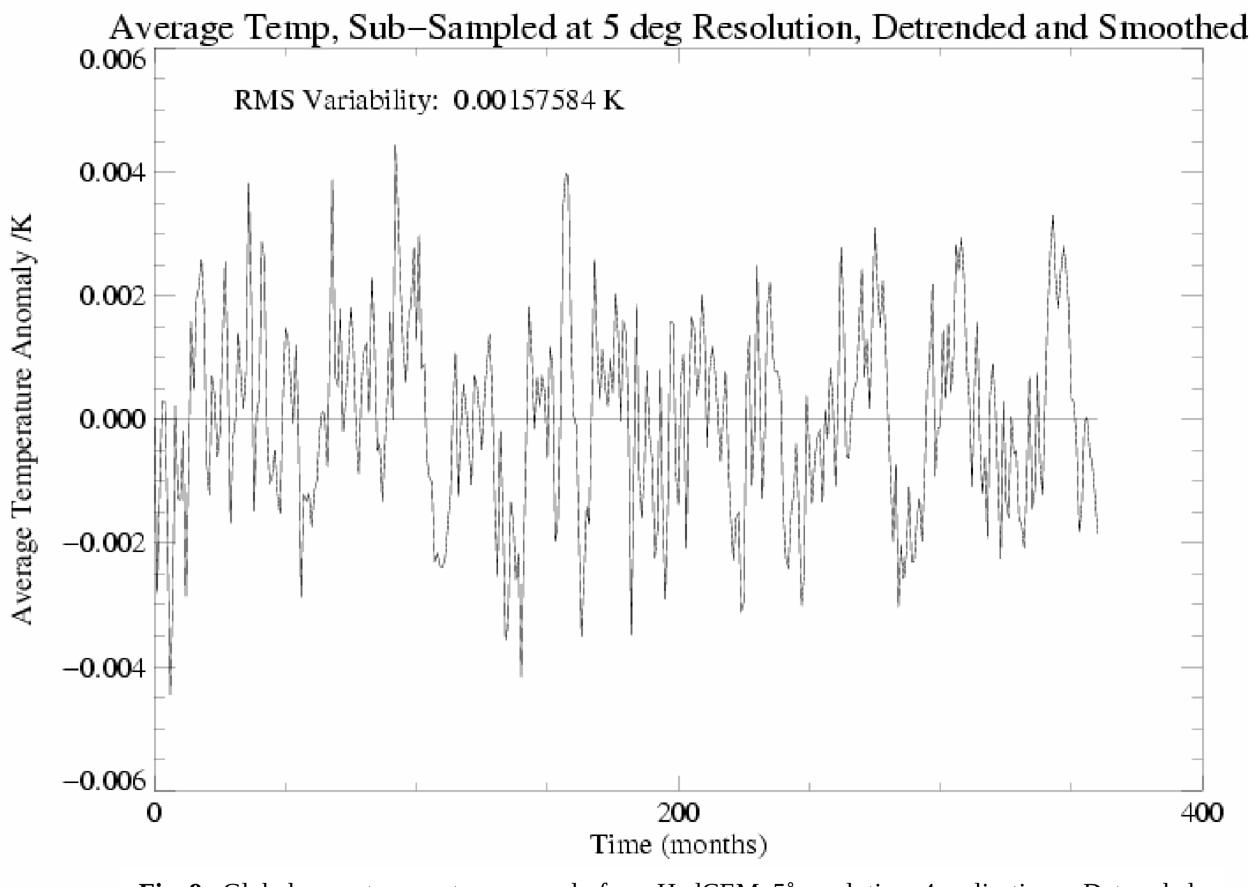

Fig. 9. Global mean temperature anomaly from HadCEM, 5˚ resolution, 4 realisations. Detrended to remove warming signal and smoothed by subtracting monthly climatology.

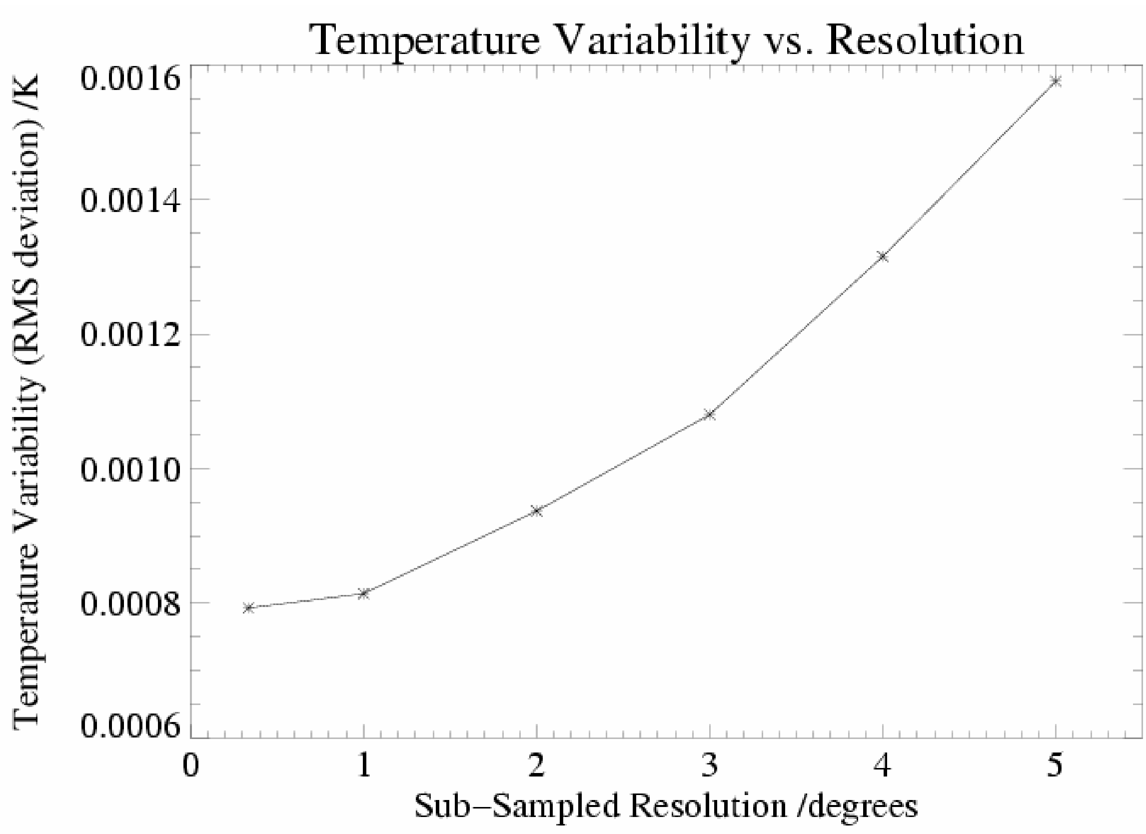

Fig. 10. RMS variability for each sub-sampled resolution.

4. Conclusions

In the first section of this report, the ocean heat content in the ENACT objective re-analysis was studied. Listed below are the main conclusions from this section.

- The trend in ocean heat content from the ENACT reanalysis was compared with previous results from Levitus and HadCM3. It was found that the warming trend over the last 50 years is comparable between the three time-series, and that the temporal variability exhibited by ENACT is similar to that seen in the Levitus results. HadCM3 does not replicate the decadal variability in heat content.

- The ENACT values of temperature were studied for separate regions of the world ocean, and for varying depths. The largest temperature trend was found in the top 100m of the ocean. The Atlantic Basin and the tropical latitudes (30˚N to 30˚S) were the regions with the largest trend.

- Regions with significant correlation with the global time-series were identified. Despite there being a relatively high sampling density in the North Atlantic, this region did not show significant correlation with the global time-series.

- The temperature variability as a function of depth was studied and compared to the Levitus results. As was the case with Levitus, variability was greatest towards the ocean surface and decayed with depth. However, the peak at a depth of 500m observed in Levitus was not apparent in the ENACT results.

- Possible effects of sparse data sampling and the ENACT data interpolation method were suggested. It is thought that areas with low sampling density may yield low values of ocean heat content. This may explain the low values found in the Southern Ocean.

The second section of this report focused on the effect of sub-sampling on the variability in a version of the climate model with an eddy-permitting ocean model.

- Investigations suggest that sampling at coarser spatial resolution, i.e. taking point measurements to be representative for larger spatial regions leads to higher temporal variability in each temperature time-series. This is consistent with the results from previous work by Palmer and Banks (2004). This effect would introduce uncertainty in the results.

Improvements and Further Work

Listed below are improvements and extensions that could be made to this work given more time.

- A spatial contour plot for variability could be constructed for the ENACT data, to determine the regions of the world ocean that are most responsible for the observed decadal variability.

- The heat content trend could be calculated for the HadCEM simulated time-series, for comparison with ENACT, Levitus and HadCM3.

- The temperature variability as a function of depth could be investigated for HadCEM, and compared to the results from ENACT, Levitus and HadCM3. This could help to identify the extent to which the results from the other three sources are influenced by the coarse sampling resolution.

- A contour plot showing values of RMS variability in HadCEM could be constructed to identify regions of the world ocean with high eddy activity. This could be used to segregate areas of the ocean which could have a higher resolution in models.

- The effect of temporal sub-sampling in HadCEM could be investigated (rather than spatial).

- The importance of the data interpolation methods could be studied by processing HadCM3 data by method used by Levitus for the WOD data.

- In the procedure to construct the ENACT objective analysis a double correction to the XBT drop-rate was applied. This will result in a (fairly small) spurious warming (down to about 600m) since 1995. This part of the analysis will be redone, at which point it would be useful to recalculate the heat content.

Acknowledgments

This work was supervised by Michael Vellinga, who I thank for his suggestions and support. I am grateful for useful discussions with Helene Banks, Bruce Ingleby and Matt Huddleston. I also thank Jonathan Gregory, Peter Stott, Sheila Stark, Yvonne Searl and Ian Culverwell for their assistance. The ENACT objective analysis was produced at the Met Office under EU FP5 contract EVK2-CT2001-00117

References

Gordon, C., C. Cooper, C. A. Senior, H. Banks, J. M. Gregory, T. C. Johns, J. F. B. Mitchell, and R. A. Wood, The simulation of SST, sea ice extents and ocean heat transports in a version of the Hadley Centre coupled model without flux adjustments, *Clim. Dyn.*, *16*, 147–168, 2000.

Gregory, J. M., H. T. Banks, P. A. Stott, J. A. Lowe and M. D. Palmer, Simulated and observed decadal variability in ocean heat content, *Geophys. Res. Lett. ,31*, L15312, doi:10.1029/2004GL020258., 2004.

Ingleby, B. and Huddleston, M. Quality control of ocean profiles - historical and real-time data., *subm. to Journal of Marine Systems*, 2004.

Levitus, S., J. I. Antonov, T. P. Boyer and C. Stephens, Warming of the World Ocean, *Science*, *287*, 2225-2229, 2000.

Palmer, M. D. and H. T. Banks, Evaluation of ocean heat content in the HadCM3 coupled ocean-atmosphere model compared with observations and the effect of sampling, Unpublished Hadley Centre Manuscript, 2004.

Roberts, M. J., H. Banks, N. Gedney, J. Gregory, R. Hill, S. Mullerworth, A. Pardaens, G. Rickard, R. Thorpe and R. Wood, Impact of an Eddy-Permitting Ocean Resolution on Control and Climate Change Simulations with a Global Coupled GCM, *J. Climate, 17,* 3-20, 2004.